ELSEVIER

Coordination Chemistry Reviews
171 (1998) 365–386

COORDINATION CHEMISTRY REVIEWS

Toward transparent molecular wires: electron and energy transfer in transition metal derivatized conducting polymers

Biwang Jiang, Szu Wei Yang, Scott L. Bailey, Leone G. Hermans, Ross A. Niver, Milissa A. Bolcar, Wayne E. Jones, Jr. *

Department of Chemistry, Institute for Materials Research, and Integrated Electronics and Engineering Center, Binghamton University, Binghamton, NY 13902-6016, USA

Received 7 July 1997; accepted 19 November 1997

Contents

* Corresponding author.

PII S0010-8545(98)00032-0

Abstract

A great deal of research has concentrated on long range electron and energy transport in transition metal-based systems, including molecular donor–acceptor assemblies, electron and energy transfer cascades, dendrimers, and derivatized polymer systems. In an effort to improve efficiencies for electron and energy transport over large distances, several groups have now turned to conjugated systems. Several challenges exist to incorporating conducting materials/polymers in the study of photoinduced electron and energy transfer: solubility and processibility of the materials, thermal stability and limitations on direct spectroscopic characterization due to band gap absorptions. We have prepared a new series of conducting materials that provides for direct incorporation of chromophores and electrophores within the backbone of a conducting polymer. Energy transfer dynamics between conducting polymer bridges and porphyrin or metal-to-ligand charge transfer (MLCT) chromophores can be controlled through intermolecular interactions in solid vs solution samples. We have also developed a methodology to incorporate transmissive benzothiophene-type polymers such as polyisothianaphthene (PITN) within a copolymer assembly. These new materials are now being used to investigate long range electronic coupling and have potential applications that range from artificial photosynthesis to light emitting diodes. © 1998 Elsevier Science S.A.

Keywords: Electron transfer; Energy transfer; Electronic coupling

1. Introduction

Electronic communication in extended materials represents a challenging and interdisciplinary research area [1–22]. In recent years, numerous new materials have been developed for applications that range from electro-optic devices [19–22] to artificial photosynthesis [1–18]. The goal in these materials is to create supramolecular complexes that when irradiated with electromagnetic radiation will undergo electron and energy transfer processes that result in controlled and useful changes in the material. By combining inorganic photochemistry with recent developments in conducting polymer chemistry [23–26], we are seeking to create photoactive copolymers that will provide further insight into the dynamics of long range electronic coupling.

1.1. Energy transfer and charge separation models

Long range electron and energy transfer in molecular systems is best exemplified by the photochemistry of the reaction center in the photosynthetic assembly [1–8]. Following excitation, a series of energy and electron transfer events occurs within several hundred picoseconds that separates electrons and holes within a molecular architecture. Given the high efficiency of the natural system, a great deal of effort has gone into understanding the fundamental processes involved in the electron and energy transfer events [1–5]. In addition, theoretical studies and experiments involving model complexes have provided a critical basis for our understanding of electronic coupling in these extended systems [10–22,27].

Typical artificial photosynthetic assemblies incorporate a series of energy and electron transfer events from donors, D, to acceptors, A, that separate a charge over a large distance (Fig. 1(a)) [5,7,8,16–18]. The advantage of this system is a substantial decrease in the rate of energy-wasting back electron transfer. The disadvantage is the resulting loss in available free energy, ΔG, that results from the cascading electron transfer events. A more effective method of separating charge would be to incorporate a degenerate set of orbitals that would provide for redistribution of electron density from D to A without a significant decrease in available free energy (Fig. 1(b)).

There are several examples in the literature of newly-created model dimeric structures that involve conjugated bridges in the context of the donor–acceptor model system [10–18,27–30]. Dimer studies are limited by the relatively small distances of charge separation that can be achieved and by the single electron transfer events that occur. Photosynthesis often involves multiple electron transfer events. Recently, several groups have extended this technology to create multi-chromophoric arrays [10–15,19–22] and derivatized polymers [9,27–30].

1.2. Conducting polymers

Electrical conductivity in extended conjugated systems has been known for over 20 years [31]. Preparation of organic structures where conjugation extends over hundreds of monomer units such as thiophene, pyrrole or acetylene, results in electronic communication and conduction that is as efficient as metallic conductors such as copper, e.g. 10^5 S cm^{-1} [31]. By combining recent synthetic methodologies we can create "molecular wires" that interconnect multiple chromophores and quenchers within a single molecular framework.

A drawback to the use of many conjugated polymers in photoinduced electron transfer is that they are themselves strongly colored [32]. Bandgap transitions typically occur in the visible region of the spectrum, thereby decreasing the quantum yield in photoexcitation experiments and limiting spectroscopic characterization of the excited state and electron transfer products. A solution to this problem would be to adjust the bandgap transition to lower energies, e.g. to the near IR, and this

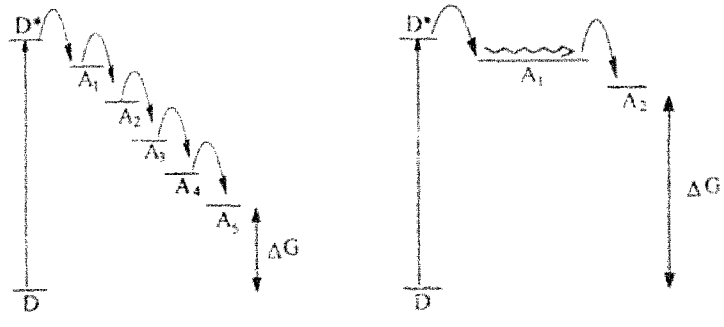

Fig. 1. State diagrams for energy transfer through an electron transfer cascade and through a conjugated π-system

has recently been achieved in the form of a polybenzo[*c*]thiophene conjugated polymer [33,34]. The observation of transmissive behavior in a conjugated system thus provides an opportunity to overcome the optical limitations of conducting polymers.

In the work summarized here we have prepared several new conjugated systems that systematically incorporate transition metal-based chromophores within the conjugation of extended π-systems. We have included both derivatized porphyrins (M=Zn, Ni, Cu, and free base) and metal-to-ligand charge transfer (MLCT) complexes (M=Ru; L=4,4′-dimethyl-2,2′-bipyridine, terpyridine) as the chromophores in these systems, shown below. Finally, we have extended our efforts on conducting polymer systems to include derivatized polyisothianaphthene (PITN, *vide infra*).

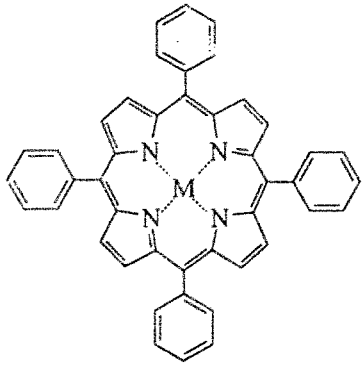

Porphyrin Monomer

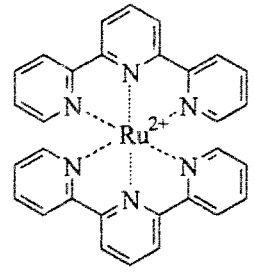

Ruthenium Terpyridine Complex

2. Porphyrin copolymers

2.1. Synthetic strategies

The Wittig reaction has been widely used to synthesize conjugated conducting polymers [35,36]. Recently, this reaction has also been used in constructing porphyrin dimers, trimers and a star-like pentamer [37–39]. By further exploration of this methodology, we have synthesized linear, conjugated porphyrin polymers as depicted in Scheme 1 [40]. The key to the preparation of these polymers is the synthesis of the appropriately-functionalized porphyrin phosphonium salts **2**. We began with the synthesis of 5,15,-bis(chloromethylphenyl)-10,20-bis(mesityl)porphyrin **1** [41], and then the porphyrin phosphonium salts were prepared by reaction of **1** with triphenyl phosphine (PPh_3). The Wittig reaction of the porphyrin phosphonium salt and various oligophenylenevinylene dialdehydes [40] led to porphyrin polymers with different linkage lengths (**FbPP3**, **FbPP5**, **FbPP9**).

There are several distinct advantages to these new polymer systems for the study

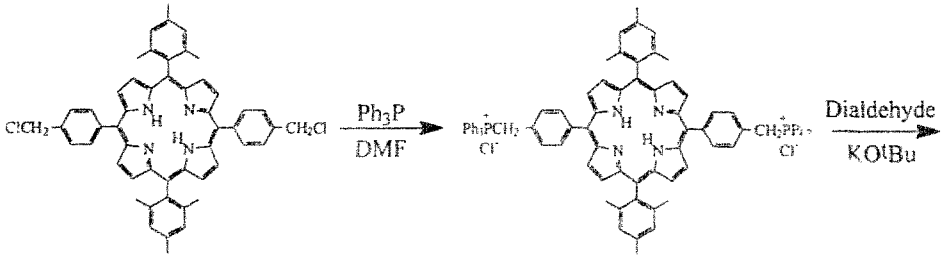

1 2

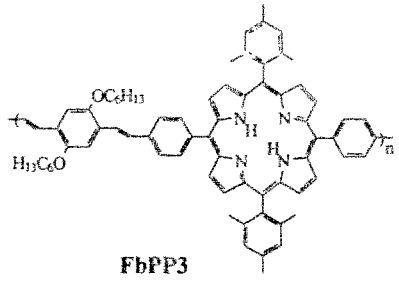

FbPP3

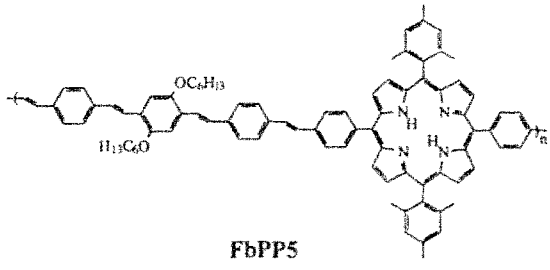

FbPP5

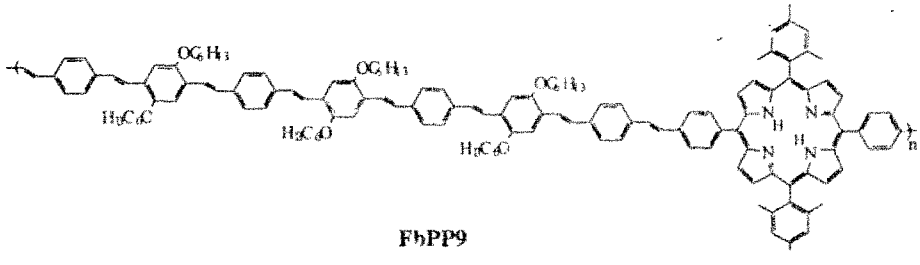

FbPP9

Scheme 1. Synthetic scheme for porphyrin monomers and polymers.

of electron and energy transfer. The reaction is facile even under room temperature conditions, making modification of the polymer and chromophore readily accessible. The solubility of the porphyrin copolymers is substantially increased due to the long

alkoxyl substituents attached to the oligophenylenevinylene units. This is a common strategy in the synthesis of soluble polymers [35,36,42]. Based on recent work by Lindsey and coworkers, mesityl substituents on porphyrin rings also contribute to the solubility of multi-porphyrin arrays [10–15]. Finally, the thermal stability of the polymer in the solid state was enhanced over pure polyphenylenevinylene (PPV) polymer systems based on DSC and TGA measurements [40,41].

The favorable solubility of the new porphyrin polymers provided for extensive characterization by traditional spectroscopies (e.g. NMR, IR) that verified the repeat units represented in Scheme 1 and the all-*trans* configuration of the oligophenylenevinylene bridges. GPC (relative to polystyrene standards) and light-scattering measurements indicated a number average molecular weight (M_n) of approximately 13 000 for all of the systems, corresponding to degrees of polymerization that would contain more than 12 chromophores on each polymer strand.

2.2. *Solution photophysics*

UV-vis spectra for a representative polymer and porphyrin monomer in THF solution are shown in Fig. 2. The absorption maxima of the porphyrin Soret bands (422 nm) were all slightly red shifted and broader than that of the corresponding porphyrin monomer (maximum absorption at 418 nm) due to π-conjugation effects [43]. However, there was no significant difference in the UV-vis spectra as a function of the length of π-conjugation in the bridge. No splitting of the Soret bands was observed, suggesting that there may be limited ground-state electronic interaction between the porphyrin units in solution [37], though a lack of splitting does not preclude electronic communication [10–15].

The fluorescence spectra (422 nm excitation) of the polymers in THF solution are shown in Fig. 3 (top). Two emission manifolds are observed. The low energy bands (640–750 nm) are independent of the length of oligophenylenevinylene bridges and have an emission lifetime of 11.5 ± 0.3 and 1.9 ± 0.3 ns for the free base and Zn

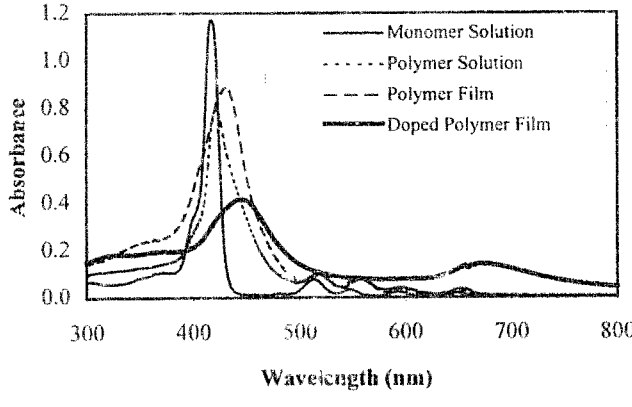

Fig. 2. UV-vis spectra of **FbPP3** in solution and as a film in the doped or undoped state compared with the porphyrin monomer.

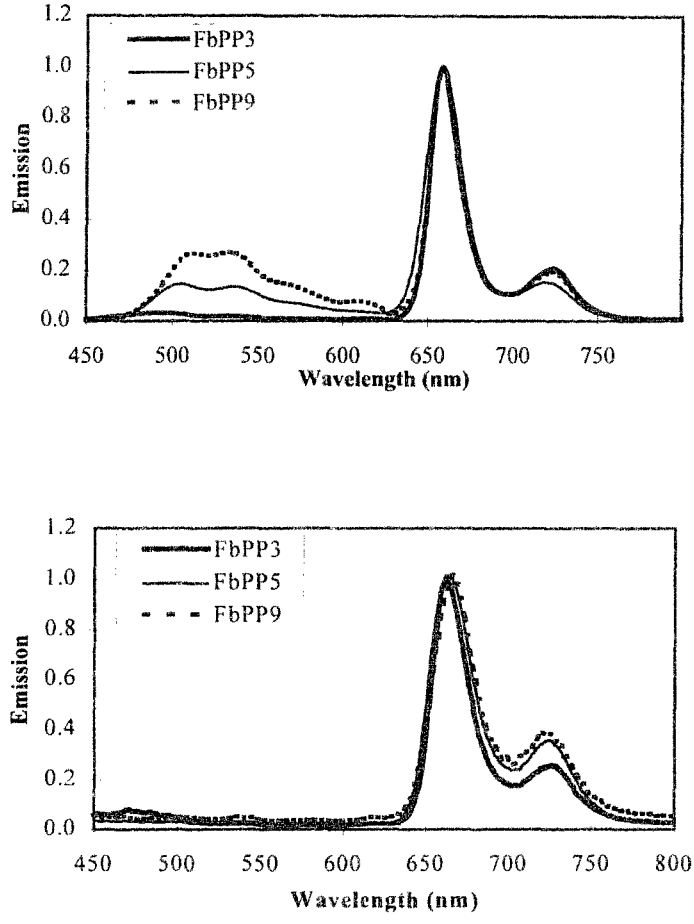

Fig. 3. Emission spectra of polymers in THF (top) and as solid films (bottom) (422 nm excitation).

chromophores, respectively. These low energy features can be attributed to the porphyrin subunits within the polymer chain, based on similarity to the monomer fluorescence properties and comparison of excitation and absorption spectra. The higher energy emission bands (450–600 nm) increase in intensity and red shift with increasing conjugated bridge length. These features can be assigned to the oligophenylenevinylene bridge, based on model studies of the bridge prior to polymerization. The emission lifetime of this higher energy state, monitored at 560 nm, was 500 ps for the Fb**PP9** system. The quantum yield of the emission was also enhanced as the bridge length increased: $\Phi_{em}=0.10$, 0.13 and 0.23 for Fb**PP3**, Fb**PP5** and Fb**PP9**, respectively [44]. The increase in the emission quantum yield was dominated by the observed emission from the bridge, though there was a slight increase in emission quantum yield from just the porphyrin band relative to the monomer ($\Phi_{em,porph}=0.10$, 0.11, 0.15 and 0.02 for Fb**PP3**, Fb**PP5**, Fb**PP9**, and the monomer, respectively) [44].

2.3. Solid state photophysics

Given the extensive solubility of these new materials in organic solvents, high quality thin films could be obtained by spin casting 0.1M toluene solutions of the polymers onto glass slides. Shown in Fig. 2 are the UV-vis absorption spectra of a representative doped (*vide infra*) and undoped polymer film (**PP3**). The maximum absorption of the undoped film at 430 nm was significantly red shifted compared to the spectra in THF solution. After chemical doping with nitromethane solutions of anhydrous $FeCl_3$, a new broad-band absorption feature appears at low energy, consistent with formation of a bandgap in the conducting form of the polymer [31]. The undoped films were completely insulating, with conductivities less than 10^{-12} S cm^{-1} as measured by the in-line four-probe method [45]. After doping, the conductivity of the film increased significantly to $\sim 10^{-6}$ S cm^{-1}. Previously, we demonstrated that conductivities as high as 10^{0} S cm^{-1} can be achieved at lower concentrations of porphyrin in PPV polymer systems [41].

There was a significant shift in the emission intensities of the polymers when cast as thin films, Fig. 3 (bottom). The thin film fluorescence spectra are dominated by the porphyrin bands at low energy with a slight red shift from the solution spectra. Emission lifetimes were substantially increased ($\tau > 500$ ns) in the solid state. Noticeably absent in the thin film spectra are the emission bands at higher energy associated with the oligophenylenevinylene bridge.

2.4. Energy transfer

One conclusion that could be drawn from the absorption and emission data above is that energy transfer from the higher energy bridge state to the lower energy porphyrin units was taking place in the solid state, but not in solution. Further support for this conclusion is found by comparing the absorption spectra to the excitation spectra in both the solution and solid state. The results of fluorescence excitation experiments in solution, monitoring the emission either at 550 or 724 nm, show that the absorptions which lead to the two emissions are consistent with the bridge and monomer absorption spectra, respectively. In the solid state, the fluorescence excitation spectrum of the low energy band (724 nm) overlaps completely with the UV-vis spectrum of the polymer. Based on these results, we conclude that energy transfer between the bridge and porphyrin subunits is inefficient at low concentration in solution.

One possible explanation for the weak intramolecular communication in solution is that steric hindrance between the β-pyrrole proton of the porphyrin and the *ortho* proton of the bridge phenyl group forces the porphyrin rings out of the plane of conjugation in solution (Fig. 4). This has been observed previously for phenyl-substituted porphyrin dimers and oligomers [10–15]. This explanation is also consistent with preliminary molecular modeling work which shows that the oligophenylene bridges are found to adopt helical structures due to steric interactions between the long alkyl chains [50]. In either case, the decrease in conjugation through the extended system could result in the dual excited state emission observed in solution.

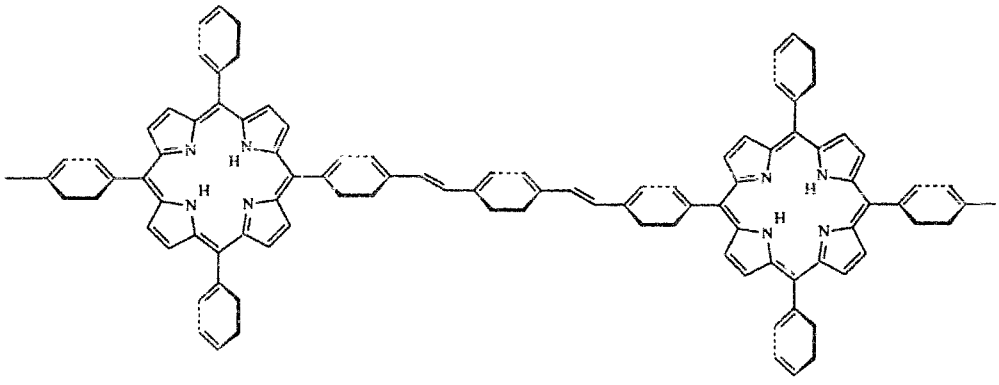

Fig. 4. Nonplanar structure of porphyrin polymer.

In the solid state there is enhanced electronic communication, leading to energy transfer from the higher energy bridge to the porphyrins. A possible explanation of this effect is that in the solid state the porphyrin subunits are preferentially stacking [46,47]. This stacking would force the porphyrin rings to be within the same plane as the conjugated bridge in the solid state leading to enhanced *intrastrand* electronic coupling. While it could be argued that this type of interaction would lead to self-quenching of the porphyrin emission [48,49], it has previously been shown that solid state π-stacking of porphyrins can result in enhancement of the emission quantum yield compared to solution [46]. Preliminary X-ray diffraction results on these polymer films show that they exhibit short range order within the films.

An alternative hypothesis would be that in the solid state an increase in *interstrand* energy transfer leads to the observed decrease in emission intensity from the bridge-based state. Monitoring the emission of dilute solid samples of the Fb**PP9** polymer in polystyrene or polymethylmethacrylate matrices reveals a substantial increase in the bridge-based emission with decreasing concentrations of the Fb**PP9** polymer

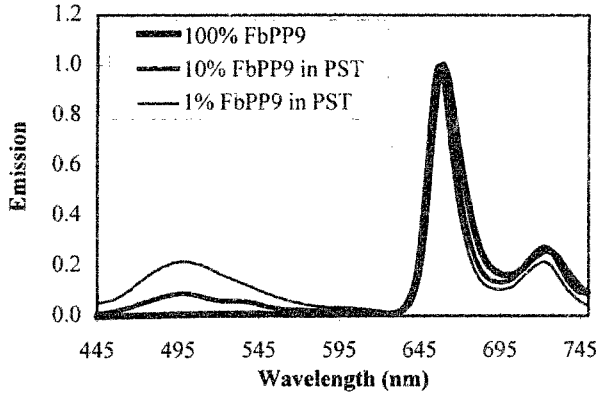

Fig. 5. Solid state emission spectra of **FbPP9** in a polystyrene (PST) matrix (422 nm excitation).

(Fig. 5). This inverse relationship suggests that the process leading to the observed loss of the dual emission is intermolecular in nature.

3. Donor–acceptor copolymers

A better measure of electronic coupling through these conjugated porphyrin copolymer systems would be to explore interactions between two different chromophores within the same conjugated chain. This has recently been achieved by preparing heteroporphyrin polymers in which the porphyrin was varied from the free base to M = Zn, Ni and Cu [50].

3.1. Synthetic strategies

The key to the design and synthesis of an alternating hetero-metalloporphyrin polymer is the availability of the porphyrin monomer **3**, shown in Scheme 2. There are two remarkable features of this porphyrin monomer: The first is that it possesses reactive aldehyde substituents which can be coupled with another porphyrin diphosphonium salt. The second is its high solubility due to the hexyloxy substituent on the phenylvinylene moiety. The reaction of porphyrin diphosphonium salt **2** with excess 2,5-diformyl-1,4-dihexyloxybenzene led to a *cis,trans*-vinylene isomer of monomer **3a**. Interestingly, metallation with zinc acetate in refluxing $CHCl_3$/methanol led to nearly quantitative formation of the *trans*-metalloporphyrin, **3b**, as measured by ^1H NMR. The isomerization mechanism is unclear at present, and further exploration is necessary.

The reaction of metalloporphyrin dialdehyde **3a** and free base porphyrin diphosphonium salt **2** initially yielded a hybrid polymer with alternating Zn–porphyrin and free base porphyrin units (**ZnFbPP3**, Scheme 2). This hybrid Zn–Fb polymer can be further metallated by a second metal ion such as Cu(II) or Ni(II) to give the heterometallated porphyrin polymers **ZnCuPP3** and **ZnNiPP3**. The insertion of the second metal ion was monitored by UV-vis absorption, and the spectra for each polymer in THF solution are shown in Fig. 6. All these porphyrin polymers are highly soluble in common organic solvents such as chloroform and THF, which facilitates spectroscopic characterization. The structure determined by NMR and shown in Scheme 2 is supported by subsequent metallation of **ZnFbPP3** with zinc acetate to give the exact same ^1H NMR spectrum as **ZnPP3** or by demetallation to give the same ^1H NMR spectrum as the free base porphyrin polymer **FbPP3**. GPC (versus polystyrene standards) in THF indicated a molecular weight (M_n) of 12 500 with a polydispersity of 1.8, corresponding to approximately six repeat units (12 porphyrin units).

3.2. Solution photophysics

The electronic absorption spectra of the hybrid porphyrin polymers (**ZnFbPP3**, **ZnNiPP3**, **ZnCuPP3**), the free base porphyrin polymer (**FbPP3**) and the Zn porphy-

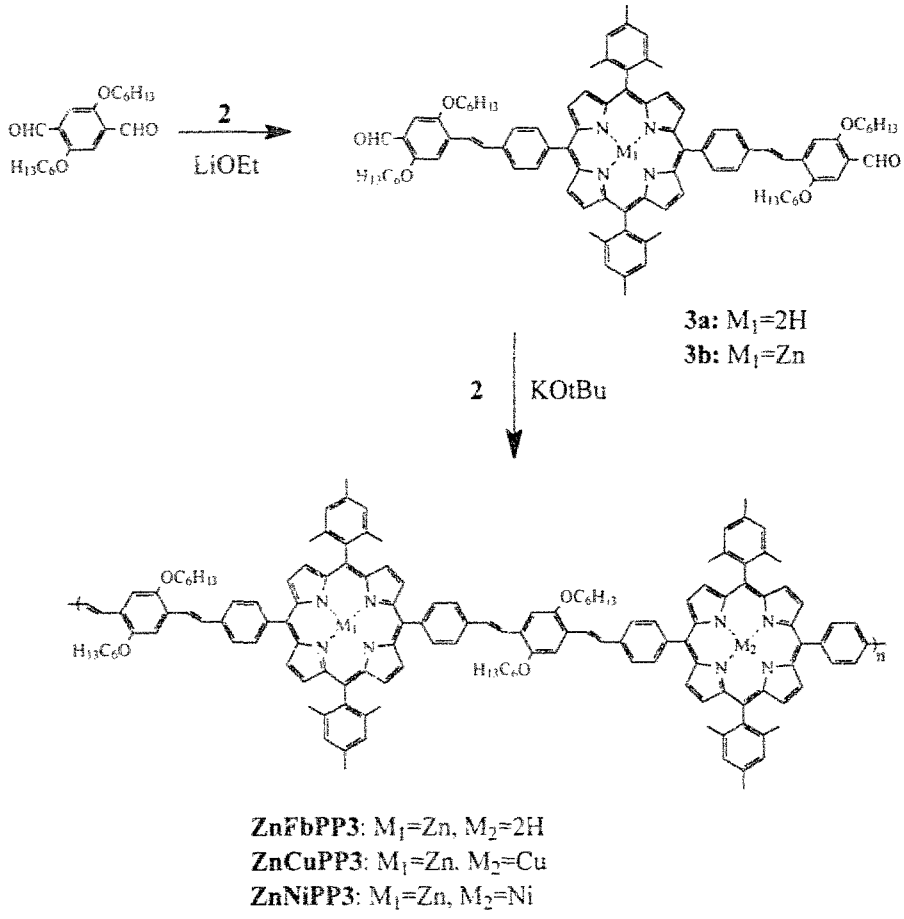

Scheme 2. Synthetic scheme for hybrid porphyrin polymers.

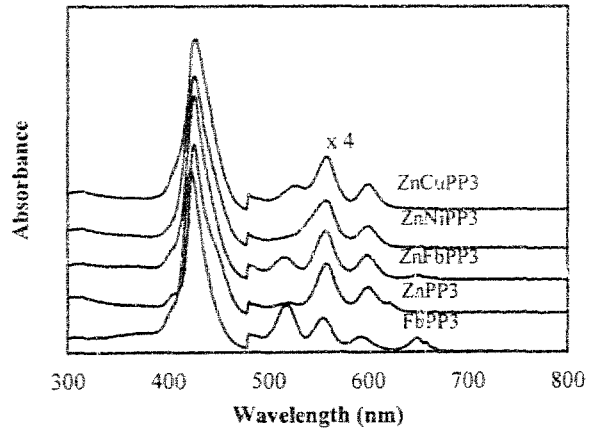

Fig. 6. UV-vis spectra of hybrid polymers and homopolymers in THF solution.

Table 1
Porphyrin polymer spectral parameters (λ in nm)

Polymers	Absorption λ_{max} (ϵ, $cm^{-1} M^{-1}$) (toluene)	Absorption λ_{max} (film)	Emission λ_{max}	λ_{sh}	Lifetime τ (ns) ±5%	Quantum yield[b] Φ
FbPP3	422 (2.66×10^5)	430	660	774	11.7[a]	0.10
FbPP5	422 (3.13×10^5)	430	660	774	11.3	0.13
FbPP9	426 (3.38×10^5)	430	615	774	11.5	0.24
ZnPP3	426 (3.10×10^5)	434	615	665	1.9	0.07
ZnPP5	426	438	615	665	1.9	0.09
ZnPP9	426	442	615	665	2.5	0.18

[a] The lifetime was determined in the presence of a very short-lived component (ps) due to the oligophenylene bridge.
[b] Quantum yields were measured agaist ZnTPP (0.033) in toluene.

rin polymer (**ZnPP3**) are shown in Fig. 6. The absorption spectra of these porphyrin polymers have similar absorption maxima to that of the corresponding porphyrin monomers. The absorption bands of the polymers are much broader, however, than those of the monomer, consistent with increased delocalization in the excited state [10–15]. The absorption spectrum of **ZnFbPP3** is essentially a superposition of **FbPP3** and **ZnPP3**, particularly clear for the B-band absorptions at low energy. This suggests limited electronic interaction between the porphyrin units in the ground state [51].

The absorption and emission spectral parameters for the donor–acceptor system and model copolymers are listed in Table 1. There was no evidence for bridge-based fluorescence from these systems, consistent with the shorter bridge length used here. The fluorescence spectrum of the **ZnFbPP3** donor–acceptor copolymer is not a superposition of the two emission manifolds. A comparison of the fluorescence spectra of **ZnFbPP3** and an equimolar mixture of **ZnPP3** and **FbPP3** (Fig. 7) clearly shows that there is a substantial decrease in the emission intensity from the higher energy **ZnPP3** chromophore relative to the lower energy **FbPP3**. Monitoring the

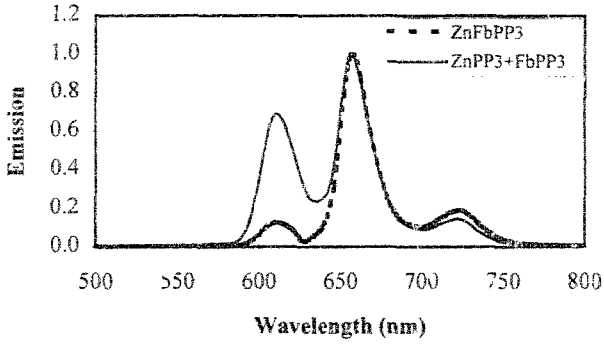

Fig. 7. Emission spectra of hybrid polymer **ZnFbPP3** and equimolar mixture of homopolymers **ZnPP3** and **FbPP3** in THF solution (422 nm excitation).

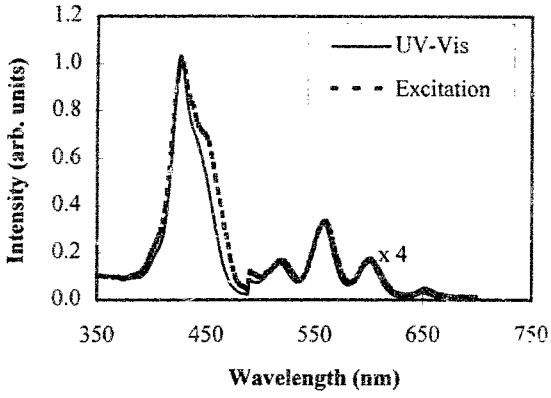

Fig. 8. Excitation spectrum of **ZnFbPP3** (monitored at 724 nm) compared with UV-vis spectrum of **ZnFbPP3**.

emission at 724 nm, the excitation spectrum is found to overlap completely with both the Zn and Fb portions of the **ZnFbPP3** absorption manifold, Fig. 8.

The results of frequency-domain emission lifetime measurements in THF solution are shown in Table 2. By comparison to the monomer and the model copolymers above, we can clearly assign the 1.8 and 10.1 ns components to fluorescence from the Zn and free base porphyrins, respectively. In the case of the donor–acceptor hybrid polymer system, a small amount of an additional short-lived component is observed with a lifetime of ~240 ps.

3.3. Energy transfer

Based on the combined fluorescence results above, we conclude that following excitation, energy transfer occurs from the higher lying Zn π–π^* state to the free base. The mechanism of this energy transfer process may or may not include the participation of the PPV bridge. In previous investigations on porphyrin dimers, several groups have demonstrated that rapid energy transfer can occur through a Förster-type mechanism [10–22,51–53]. This mechanism would not require direct electronic coupling. Given the limited electronic coupling observed between the porphyrins and the conjugated **PP5** and **PP9** bridges above, it is also likely that a

Table 2
Porphyrin polymer spectral parameters (λ in nm), all in THF solution

Polymer	Absorption (λ_{max})	Emission (λ_{max})	τ (ns)
FbPP3	422	660	11.75
ZnPP3	426	615	1.93
ZnFbPP3	426	615, 660	10.10, 1.83[a]

[a] A fast component with a lifetime of ~240 ps was also observed, but could not be quantified.

Förster mechanism is involved here. As expected based on the model compounds, the solid state fluorescence data are also consistent with rapid energy transfer.

The energy transfer process is not complete in room temperature solution. As shown in the emission spectra, we determined that ~10% of the emission remained in the Zn porphyrin unit. However, the residual emission from the Zn porphyrin state was single exponential. This would suggest that there is some non-uniformity in the copolymer structure. This structural distortion was not evident in emission from solid state samples that demonstrated complete energy transfer to the free base acceptor. The small percentage of very short-lived emission that was observed can be assigned to the energy transfer rate based on time-resolved emission measurements. Thus, we believe that energy transfer is rapid with $k \sim 4 \times 10^9\ s^{-1}$.

4. Photoinduced electron transfer in conducting polymers

A unique property of conductive polymers is the reversible switching that occurs between the nonconducting and the conducting forms via oxidation and reduction, or protonation and deprotonation, as shown in Eq. (1) [31,54,55].

$$(C)_x^+A^- + e^- \rightleftharpoons (C)_x + A^- \quad (1)$$

In Eq. (1), C is the conductive polymer containing cationic radicals stabilized over x units, and A is the counter ion that is used to maintain charge neutrality. The formation of radical cations in this way can lead to charge defects giving rise to bipolaron (bivalent cation for a two electron loss) energy levels responsible for conduction [32,56].

The creation of charged species in conjugated systems can also be described using a donor–acceptor model which employs charge transfer assemblies. For example, a model has recently been reported involving a reversible charge transfer that utilizes molecular oxygen as the acceptor and poly(3-alkylthiophene) as the donor [57]. Other approaches towards the use of donor–acceptor systems involving conjugated polymers include the use of chromophores which have demonstrated photoinduced energy transfer [27,58] and both inter- and intramolecular electron transfer [23,24] involving pendant groups to the polymer chain [9,59,60].

It is also possible to use photoinduced charge transfer reactions to reversibly oxidize the conjugated polymer. By careful selection of excited state oxidation and reduction potentials, a chromophore/conducting polymer system can be prepared where initial excitation into the chromophore results in an increase in charge carriers and a change in the conductivity as shown in Eq. (1). Heeger et al. first demonstrated a working system based on this premise [23–26]. It possessed a conjugated polymer as a chromophore that exhibited photoinduced electron transfer to a C_{60} electron trap.

A more efficient system would employ a chromophore with a long-lived excited state that was capable of excited state electron transfer to form the oxidized polymer directly. A key example would involve excitation into the MLCT band of

$[Ru(dmb)_3]^{2+}$ (dmb = 4,4′-dimethyl-2,2′-bipyridine) which results in an excited state reduction potential of +0.66 V vs SCE in chloroform [61]. The oxidation potential required to switch the emeraldine base form (EB) of either polyaniline ($PANi_{(EB)}$) or poly(2,5-dimethoxyaniline) ($PDMA_{(EB)}$) to the conductive form is approximately +0.40 V vs SCE [62]. Thus, the photoinduced oxidation of $PANi_{(EB)}$ by $[Ru(dmb)_3]^{2+*}$ is thermodynamically feasible according to the excited state reaction as illustrated in Eq. (2) below.

$$Ru^{2+} + h\nu \rightarrow Ru^{2+*} + PANi_{(EB)} \rightarrow Ru^{+} + PANi^{+} \quad (2)$$

4.1. Electron transfer quenching

The conjugated polymers $PANi_{(EB)}$ and $PDMA_{(EB)}$ can be readily synthesized and characterized according to literature methods [63,64]. Stern–Volmer analysis of the emission spectrum of $[Ru(dmb)_3]^{2+*}$ at 612 nm as a function of increasing $PDMA_{(EB)}$ concentration, Fig. 9, clearly demonstrates that the conjugated polymer system is capable of quenching the MLCT state. In this experiment, the emission intensities were corrected for the small amount of competitive absorption at 458 nm from the polymer, and pure polymer samples demonstrated no measurable luminescence. The quenching rate constant, k_q, was calculated to be $\sim 10^8 M^{-1} s^{-1}$ without adjusting for the radius of gyration of the polymer in solution [65].

Transient absorption spectroscopy on dilute chloroform solutions of 2.4×10^{-5}M $[Ru(dmb)_3]^{2+}$ and 8×10^{-4}M $PDMA_{(EB)}$ excited at 532 nm (5 mJ; 6 ns

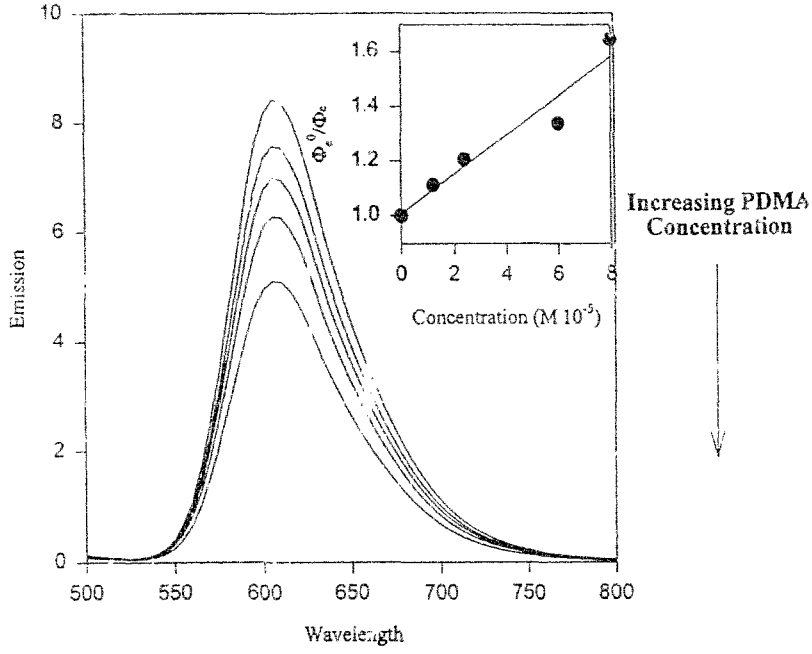

Fig. 9. Emission spectra of $[Ru(dmb)_3]^{2+}$ and PDMA in $CHCl_3$ solution.

pulses) showed a decrease in absorption at 600+ nm consistent with loss of absorption from the PDMA in this region. This loss of absorption would be consistent with Eq. (2) and an electron transfer mechanism to yield the conducting form of the polymer, $PDMA^+$ [66,67].

4.2. Photoconductivity

Solid, thin film samples were prepared by mixing 1–30% by weight of the chromophore, $[Ru(dmb)_3](PF_6)_2$ [68], with the polymer. The samples were homogenized by co-grinding, and a free-standing pellet was prepared in a die press (3.87×10^5 kPa). Resistance measurements of the solid samples under varying illumination conditions were obtained using the in-line four-probe method under dry nitrogen [45]. Initial resistance measurements were made under dark conditions at ambient temperature and showed conductivities of $>10^{-5}$ S cm^{-1}. A decrease in the resistance of the $[Ru(dmb)_3]^{2+}/PANi_{(EB)}$ mixtures was observed when the samples were excited using visible light (150 W Xe lamp). The decrease in resistance was found to be linear over one order of magnitude change in light intensity, Fig. 10. Resistance changes of greater than one order of magnitude have been achieved depending on the original resistance of the sample [69,70]. The change in resistance was completely reversible, returning to the original, pre-excitation resistance within several seconds. The time-resolved characteristics of the change in resistance are shown in Fig. 11. Following excitation, a complex rise and decay are observed which could only be fit by a multi-exponential analysis.

The theory of photoconductivity describes the change in conductivity under the action of light (Eq. (3)) where $\Delta\sigma$ is the change in conductivity, e is the charge of

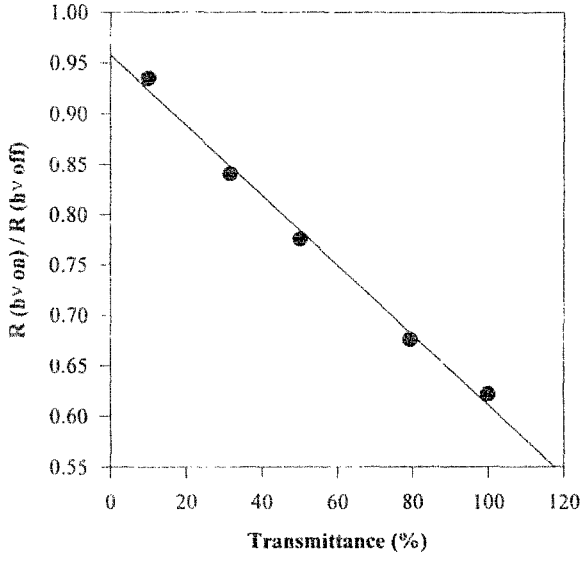

Fig. 10. Resistance vs percent transmittance for 10% $[Ru(dmb)_3]^{2+}$ in $PANi_{(EB)}$.

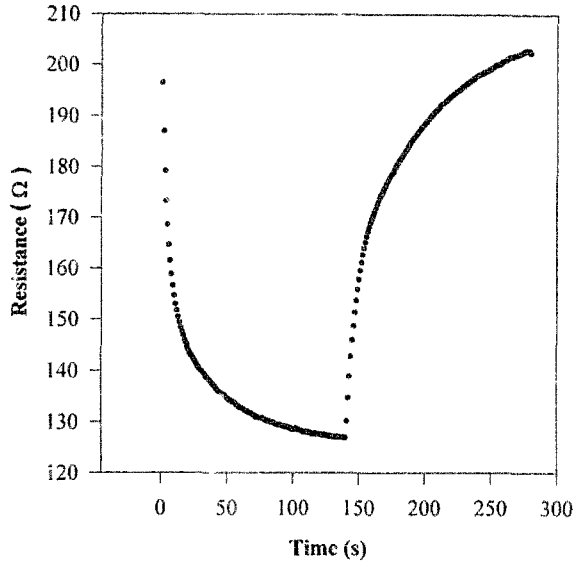

Fig. 11. Time-resolved resistance measurements.

the electron, $\Delta\mu$ is the carrier mobility, and Δn or Δp are the change in the electron or hole concentrations, respectively [71].

$$\Delta\sigma = e(\Delta\mu_n \Delta n + \Delta\mu_p \Delta p) \tag{3}$$

One possible source of the change in resistance observed following excitation involves an increased sample temperature due to light absorption. This would lead to an increase in carrier mobility. Given the relatively small temperature changes observed during the illumination period (from 297 to 305 K) and control experiments monitored in the dark over the temperature range of 293–318 K, we concluded that temperature alone is not sufficient to account for the change in resistance [69,70]. Further evidence that the decrease in resistance is not due to a thermal effect in $PANi_{(EB)}$ has been reported by Misurkin and coworkers who demonstrated that heating to 340 K caused no observable change in the optical-absorption spectrum [72].

The decrease in the resistance for the $PANi_{(EB)}$ containing $[Ru(dmb)_3]^{2+}$ could also be attributed to an energy transfer from the predominantly triplet excited state [73] of the Ru chromophore to the polymer. An energy transfer process would be consistent with the observed decrease in the emission intensity of the chromophore. This is possible for the conducting polymer systems as indicated by the presence of a low energy absorption for $PANi_{(EB)}$ at $\lambda = 620$ nm that leads to the formation of a polaron band at 820 nm [66,67]. The lack of enhanced conductivity observed for direct excitation of this low energy band in $PANi_{(EB)}$ would seem to preclude the sensitized excitation as a possible mechanism for the enhanced conductivity.

We attribute the decrease of resistance in the samples containing the chromophore to an excited state intermolecular charge transfer reaction as described in Eq. (2).

This reaction mechanism would result in the formation of charge defects which enhance the overall conductivity [23,24]. Both the emission quenching experiment and the transient absorption measurements in liquid solution are consistent with the formation of charge transfer products. Due to the lack of transparency in conducting polymer systems, it is difficult to further characterize the species involved in this reversible change in conductivity. Further, the excitation of $[Ru(dmb)_3]^{2+}$ is restricted to the surface of the pellets and not the bulk sample. This results in relatively low changes in the resistance of $PANi_{(EB)}$ under illumination.

5. Transmissive copolymers

While conjugated polymer systems are attractive for long range electron and energy transfer studies, a major limitation exists in their use for fundamental studies of electron transport. In smaller molecular systems such as diads, triads and oligomers, the conjugated bridges are not of sufficient length to establish a bandgap transition. As the bridge length increases, bandgap transitions typically occur in the visible region of the spectrum, resulting in polymers that are strongly colored. In order to overcome this limitation, we have begun a series of experiments based on polybenzothiophene derivatives such as polisothianaphthene (PITN), whose resonance forms are shown below [74,75]. These materials have bandgap transitions that are in the near IR region of the electromagnetic spectrum, but still retain high conductivities ($>10^{-2}$ S cm^{-1}) [76].

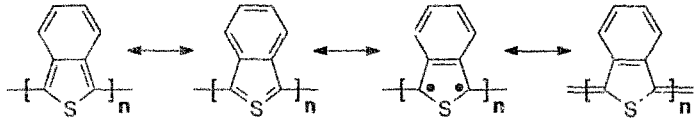

Resonance Forms of Polyisothianaphthene (PITN)

5.1. Electrocopolymerization

In order to covalently incorporate inorganic chromophores within the framework of a conducting polymer matrix, electropolymerization can be utilized. The structure of the ruthenium-based chromophore used in this experiment, $[Ru(ttpy–pyrrole)_2]^{2+}$, is shown below. $[Ru(ttpy–pyrrole)_2](PF_6)_2$ was prepared based on literature methods developed by Sauvage et al. [77]. This compound has previously been electropolymerized to form a pyrrole-based conducting polymer with pendant $[Ru(terpy)_2]^{2+}$ (terpy = 2,2′:6′,2″-terpyridine) chromophores. It has also been shown that the electrocopolymerization can be achieved in the presence of monomer pyrrole resulting in a copolymer of pyrrole and Ru-substituted pyrrole [77]. When the applied oxidation potential was relatively low (less than +0.8 V), the films consist of stoichiometric quantities of pure pyrrole [78]. This has also been achieved for polypyridyl-based polymer films [79].

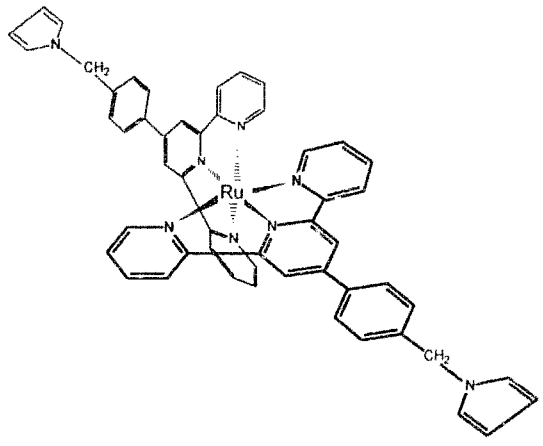

Schematic Representation of $[Ru(ttpy\text{-}pyrrole)_2]^{2+}$

5.2. *Transmissive copolymers*

The same electropolymerization technique can be applied to the copolymerization of $[Ru(ttpy\text{–}pyrrole)_2](PF_6)_2$ and the isothianaphthene monomer. Previously it has been shown that ITN will copolymerize with pyrrole [80]. In that case it was shown that the ITN monomer is covalently bound to the *ortho* position of the pyrrole. Under conditions of 10:1 molar excess of ITN in acetonitrile (with 0.1M tetrabutylammonium hexafluorophosphate as supporting electrolyte), copolymer films could be prepared on Pt electrode surfaces. The potential was held at 1.34 V vs Ag/AgCl for up to ten minutes to insure oxidation of the Ru-substituted pyrrole group and copolymerization [78].

Doping–undoping cycles of PITN are electrochemically reversible and are accompanied by an electrochromic change in the visible spectrum [81]. In the undoped state, thin films of PITN are blue; upon doping, the films become transparent. Reynolds and coworkers have also observed similar electrochromic changes in their ethylenedioxythiophene-based polymers [82–85]. By performing the copolymerization of the $[Ru(ttpy\text{–}pyrrole)_2](PF_6)_2$/ITN mixture on transparent indium tin oxide (ITO) electrodes, subsequent spectroscopic characterization can be facilitated [80]. Fig. 12 shows the UV-vis spectrum for a thin copolymer film deposited from a $[Ru(ttpy\text{–}pyrrole)_2](PF_6)_2$/ITN solution as described above. Clearly evident in the spectrum are the broad absorptions due to PITN ($\lambda_{max} = 700$ nm) and a shoulder at $\lambda_{max} = 700$ nm due to the $[Ru(ttpy\text{–}pyrrole)_2](PF_6)_2$.

Preliminary conductivity measurements on the PITN copolymers showed moderate conductivity values of 10^{-2}–10^{-4} S cm^{-1} depending on the amount of electrochemical doping [78]. Modulation of the conductivity was also observed in the presence of visible light excitation. In all cases the changes in conductivity were completely reversible. Experiments exploring the spectroscopic changes that occur following excitation are ongoing.

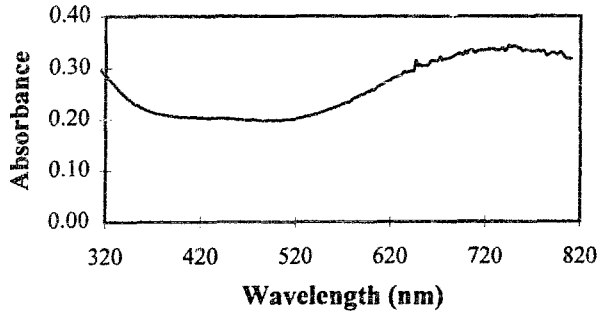

Fig. 12. Reflectance UV-vis spectrum of electrocopolymerization of $[Ru(ttpy\text{-}pyrrole)_2]^{2+}$ with ITN (1:10 molar ratio) in acetonitrile solution vs Ag/AgCl on an indium tin oxide (ITO) electrode.

6. Conclusions and future directions

The successful incorporation of transition metal chromophores into conjugated and conducting polymer systems creates several new opportunities for the investigation and application of photoinduced electron and energy transfer. The molecules described here represent examples of this new class of materials based on the systematic preparation of oligophenylene vinylene oligomers. The variety of bridges that have been created provides an opportunity to explore fundamental questions of electronic coupling in extended systems. At the same time, the optical and electronic properties of these materials make them potentially useful for LED, electro-optic and in-board resistor applications. By extending this methodology to transmissive polymers such as polyisothiaphthenes, we can overcome the limitation of overwhelmingly competitive visible light absorption in conducting polymer assemblies.

Acknowledgements

The authors wish to thank Mr. David Sarno for assistance with light-scattering measurements. This research was supported by grants from the Integrated Electronics and Engineering Center (IEEC) and the Research Foundation at the State University of New York at Binghamton. The IEEC receives funding from the NY State Science and Technology Foundation, the National Science Foundation and a consortium of industrial members.

References

[1] M.R. Wasielewski, Chem. Rev. 92 (1992) 435.
[2] V. Balzani, L. Moggi, F. Scandola, in: V. Balzani (Ed.), Supramolecular Photochemistry, Reidel, Dordrecht, 1987.
[3] H. Kurreck, M. Huber, Angew. Chem., Int. Ed. Engl. 34 (1995) 849.

[4] J. Schneider, H. Durr (Eds.), Frontiers in Supramolecular Organic Chemistry and Photochemistry, VCH, Weinheim, 1991.
[5] V. Balzani, F. Scandola, in: Supramolecular Photochemistry, Ellis Horwood, New York, 1991.
[6] H. Ringsdorf, B. Schlarb, J. Venzmer, Angew. Chem., Int. Ed. Engl. 27 (1988) 113.
[7] V. Balzani, A. Juris, M. Venturi, Chem. Rev. 96 (1996) 759.
[8] J. Sauvage, J. Collin, J. Chambron, S. Guillerez, C. Coudret, Chem. Rev. 94 (1994) 993.
[9] M.A. Fox, W.E. Jones Jr., D.M. Watkins, Chem. Eng. News 71 (11) (1993) 38.
[10] R.W. Wagner, J.S. Lindsey, J. Seth, V. Palaniappan, D.F. Bocian, J. Am. Chem. Soc. 118 (1996) 3996.
[11] R.W. Wagner, T.E. Johnson, J.S. Lindsey, J. Am. Chem. Soc. 118 (1996) 11166.
[12] J. Hsiao, B.P. Krueger, R.W. Wagner, T.E. Johnson, J.K. Delaney, D.C. Mauzerall, G.R. Fleming, J.S. Lindsey, D.F. Bocian, R.J. Donohoe, J. Am. Chem. Soc. 118 (1996) 11181.
[13] J. Seth, V. Palaniappan, R.W. Wagner, T.E. Johnson, J.S. Lindsey, D.F. Bocian, J. Am. Chem. Soc. 118 (1996) 11194.
[14] R.W. Wagner, J.S. Lindsey, J. Am. Chem. Soc. 116 (1994) 9759.
[15] R.W. Wagner, T.E. Johnson, F. Li, J.S. Lindsey, J. Org. Chem. 60 (1995) 5266.
[16] D. Gust, T.A. Moore, A.L. Moore, S. Lee, E. Bittersmann, D. Luttrull, A. Rehms, J.M. DeGraziano, X.C. Ma, F. Gao, R. Belford, T.T. Trier, Science 248 (1990) 199.
[17] D. Gust, T.A. Moore, Top. Curr. Chem. 159 (1991) 103.
[18] D. Gust, T.A. Moore, A.L. Moore, Acc. Chem. Res. 26 (1993) 198.
[19] S.M. LeCours, H. W Guan, S.G. DiMano, C.H. Wang, M.J. Therien, J. Am. Chem. Soc. 118 (1996) 1497.
[20] S. Priyadarshy, M.J. Therien, D.N. Beratan, J. Am. Chem. Soc. 118 (1996) 1504.
[21] H.L. Anderson, S.J. Martin, D.D.C. Bradley, Angew. Chem., Int. Ed. Engl. 33 (1994) 655.
[22] M.J. Crossley, P.L. Burn, J. Chem. Soc., Chem. Commun. (1991) 1569–1571.
[23] N.S. Sariciftci, L. Smilowitz, A.J. Heeger, F. Wudl, Science 258 (1992) 1474.
[24] N.S. Sariciftci, D. Braun, C. Zhang, V.I. Srdanov, A.J. Heeger, G. Stucky, F. Wudl, Appl. Phys. Lett. 62 (1993) 585.
[25] B. Kraabel, C.H. Lee, D. McBranch, D. Moses, N.S. Sariciftci, A.J. Heeger, J. Chem. Phys. Lett. 313 (1993) 389.
[26] K. Lee, R.A.J. Janssen, N.S. Sariciftci, A.J. Heeger, Phys. Rev. B 49 (1994) 5781.
[27] K. Ley, C. Whittle, M. Bartberger, M.K. Schanze, J. Am. Chem. Soc. 119 (1997) 1758.
[28] S. Boyde, G. Strouse, W.E. Jones Jr., T.J. Meyer, J. Am. Chem. Soc. 111 (1989) 7448.
[29] A. Downard, N. Surridge, S. Gould, T.J. Meyer, J. Phys. Chem. 94 (1990) 6754.
[30] T. J Meyer, Pure Appl. Chem. 58 (1986) 1193.
[31] C.K. Chiang, C.R. Fincher Jr., Y.W. Park, A.J. Heeger, H. Shirakawa, E.J. Louis, S.C. Gau, A.G. MacDiarmid, Phys. Rev. Lett. 39 (1977) 1098.
[32] M.G. Kanatzidis, Chem. Eng. News 68 (49) (1990) 36.
[33] F. Wudl, M. Kobayashi, A.J. Heeger, J. Org. Chem. 49 (1984) 3382.
[34] G. King, S.J. Higgins, J. Mater. Chem. 5 (1995) 447.
[35] J. March, I. Kang, D. Hwang, H. Shim, Macromolecules 29 (1996) 165.
[36] C. Wang, X. Xie, E. LeGoff, J.A. Thomas, C.R. Kannewurf, M.G. Kanatzidis, Synth. Met. 74 (1995) 71.
[37] D.L. Officer, A.K. Burrell, D.C.W. Reid, J. Chem. Soc., Chem. Commun. (1996) 1657.
[38] E.E. Bonfantini, D.L. Officer, Tetrahedron Lett. 34 (1993) 8531.
[39] A.K. Burrell, D.L. Officer, D.C.W. Reid, Angew. Chem., Int. Ed. Engl. 34 (1995) 900.
[40] B. Jiang, S.W. Yang, W.E. Jones Jr., Chem. Mater. 9 (1997) 2031.
[41] B. Jiang, W.E. Jones Jr., Macromolecules 30 (1997) 5575.
[42] J.H. Burroughes, D.D.C. Bradley, A.R. Brown, R.N. Marks, K. Mackay, R.H. Friend, P.L. Burn, A.B. Holmes, Nature 347 (1990) 539.
[43] N. Ono, H. Tomita, K. Maruyama, J. Chem. Soc., Perkin Trans. 1 (1992) 2453.
[44] Emission measurements and lifetimes were determined on an SLM 48000S emission lifetime fluorimeter. All solutions were bubble-deoxygenated with N_2 prior to use. Quantum yields were determined by relative actinometry using either tetraphenylporphyrin (TPP) or ZnTPP as the standard.

[45] S. Stafström, in: J.L. Brédas, R. Silbey (Eds.), Conjugated Polymers, Kluwer Academic, Dordrecht, 1991, p. 113.
[46] B. Gregg, M.A. Fox, A.J. Bard, J. Phys. Chem. 93 (1989) 4227.
[47] C.A. Hunter, J.K.M. Sanders, J. Am. Chem. Soc. 122 (1990) 5525.
[48] S.G. Boxer, Biochim. Biophys. Acta 726 (1983) 265.
[49] N.J. Turro, Modern Molecular Photochemistry, University Science Books, Mill Valley, 1991.
[50] B. Jiang, W. Jones Jr., manuscript in preparation.
[51] S. Kawabata, I. Yamazaki, Y. Nishimura, A. Osuka, J. Chem. Soc., Perkin Trans. II (1997) 479.
[52] A. Osuka, N. Tanabe, S. Kawabata, I. Yamazaki, Y. Nishimura, J. Org. Chem. 60 (1995) 7177.
[53] T. Forster, Fluorenzenz Organische Verbindungen, Vandenhoech and Ruprech, Gottingen, 1951.
[54] C.C. Han, R.L. Elsenbaumer, Synth. Met. 30 (1989) 123.
[55] A.D. Kaplin, S. Qutubuddin, J. Electrochem. Soc. 11 (1993) 3185.
[56] D.J. Sandman, Trends Polym. Sci. 2 (1994) 44.
[57] M.S.A. Abdou, F.P. Orfino, Z.W. Xie, M.J. Deen, S. Holdcroft, Adv. Mater. 6 (1994) 838.
[58] J.C. Yang, S.A. Jenekhe, Supramol. Sci. 1 (1994) 91.
[59] M. Kaneko, O. Masahisa, K. Kazuhiko, A. Yamada, J. Polym. Sci. 20 (1982) 1011.
[60] S.E. Webber, Chem. Rev. 90 (1990) 1469, and references therein.
[61] W.E. Jones Jr.., M.A. Fox, J. Phys. Chem. 98 (1994) 5095.
[62] W.E. Paul, A.J. Ricco, M.S. Wrighton, J. Phys. Chem. 89 (1985) 1441.
[63] J.C. Chiang, A. MacDiarmid, Synth. Met. 13 (1986) 193.
[64] G. Zotti, N. Comisso, G.D. Aprano, M. Leclerc, Adv. Mater. 4 (1992) 749.
[65] The quenching rate constant was limited by our knowledge of the molecular weight of the polymer. Based on the literature preparation used, the molecular weight of the polymer was 1.0×10^6 g mol^{-1} [37].
[66] Y.H. Kim, S.D. Phillips, M.J. Nowak, D. Spiegel, C.M. Foster, G. Yu, J.C. Chiang, A. Heeger, Synth. Met. 29 (1989) E291.
[67] R.P. McCall, M.G. Roe, J.M. Ginder, T. Kusumato, A.J. Epstein, G.E. Asturias, E.M. Scherr, A.G. MacDiarmid, Synth. Met. 29 (1989) E433.
[68] J.V. Caspar, T.J. Meyer, J. Am. Chem. Soc. 105 (1983) 5583.
[69] J.P. Lemmon, S.M. Gross, W.E. Jones Jr., Polym. Prep. 37 (1996) 113.
[70] J.P. Lemmon, S.M. Gross, W.E. Jones Jr., Chem. Mater. manuscript in preparation.
[71] V. Mylnikov, Adv. Polym. Sci. 115 (1994) 5–12.
[72] I.A. Misurkin, T.S. Zhuravleva, V.M. Geskin, V. Gulbinas, S. Pakalnis, V. Butvilos, Phys. Rev. B 49 (1994) 7178.
[73] The MLCT excited state of $[Ru(bpy)_3]^{2+*}$ is predominantly triplet in character and is known to sensitize the formation of organic triplet states such as anthracene. See, for example, Ref. [9].
[74] F. Wudl, M. Kobayashi, A.J. Heeger, J. Org. Chem. 49 (1984) 3382.
[75] G. King, S.J. Higgins, J. Mater. Chem. 5 (1995) 447.
[76] S.J. Higgins, C. Jones, G. King, K.H.D. Slack, S. Pétidy, Synth. Met. 78 (1996) 155.
[77] J. Sauvage, J. Collin, S. Guillerez, F. Barigelletti, L. DeCola, L. Flamigni, V. Balzani, Inorg. Chem. 30 (1991) 4230.
[78] S.L. Bailey, unpublished results.
[79] C.D. Ellis, L.D. Margerum, R.W. Murray, T.J. Meyer, Inorg. Chem. 22 (1983) 1283.
[80] M. Onada, S. Morita, H. Nakayama, K. Yoshino, Jpn. J. Appl. Phys. 32 (1993) 3534.
[81] G. Tourillon, F. Garnier, J. Phys. Chem. 87 (1983) 2289.
[82] G.A. Sotzing, J.L. Reddinger, J.R. Reynolds, P.J. Steel, Synth. Met. 84 (1997) 199.
[83] B. Sankaran, J.R. Reynolds, Macromolecules 30 (1997) 2582.
[84] G.A. Sotzing, J.R. Reynolds, P.J. Steel, Chem. Mater. 8 (1996) 882.
[85] G.A. Sotzing, J.R. Reynolds, J. Chem. Soc., Chem. Commun. (1995) 703.